ANESTHESIOLOGY

Collapse of Global Neuronal States in *Caenorhabditis elegans* under Isoflurane Anesthesia

Mehraj R. Awal, Ph.D., Gregory S. Wirak, B.S.,
Christopher V. Gabel, Ph.D.,
Christopher W. Connor, M.D., Ph.D.

ANESTHESIOLOGY 2020; 133:133–44

EDITOR'S PERSPECTIVE

What We Already Know about This Topic

- Experimental and human electrophysiologic data suggest that the anesthetic state results from a breakdown in effective communication between neurons in the central nervous system
- System-wide measurements of neuronal activity with single cell resolution under anesthesia have not been previously reported

What This Article Tells Us That Is New

- *In vivo* imaging of neuronal network activity with single cell resolution in *Caenorhabditis elegans* reveals that although neurons display highly correlated activity in awake animals, this system-wide organization in neuronal activity is lost under isoflurane anesthesia
- These observations at the single cell level in a complex neuronal network confirm previous electrophysiologic works suggesting functional disintegration of neuronal circuitry as a mechanism of anesthetic-induced unconsciousness

ABSTRACT

Background: A comprehensive understanding of how anesthetics facilitate a reversible collapse of system-wide neuronal function requires measurement of neuronal activity with single-cell resolution. Multineuron recording was performed in *Caenorhabditis elegans* to measure neuronal activity at varying depths of anesthesia. The authors hypothesized that anesthesia is characterized by dyssynchrony between neurons resulting in a collapse of organized system states.

Methods: Using light-sheet microscopy and transgenic expression of the calcium-sensitive fluorophore GCaMP6s, a majority of neurons (n = 120) in the *C. elegans* head were simultaneously imaged *in vivo* and neuronal activity was measured. Neural activity and system-wide dynamics were compared in 10 animals, progressively dosed at 0%, 4%, and 8% isoflurane. System-wide neuronal activity was analyzed using principal component analysis.

Results: Unanesthetized animals display distinct global neuronal states that are reflected in a high degree of correlation ($R = 0.196 \pm 0.070$) between neurons and low-frequency, large-amplitude neuronal dynamics. At 4% isoflurane, the average correlation between neurons is significantly diminished ($R = 0.026 \pm 0.010$; $P < 0.0001$ *vs.* unanesthetized) and neuron dynamics shift toward higher frequencies but with smaller dynamic range. At 8% isoflurane, interneuronal correlations indicate that neuronal activity remains uncoordinated ($R = 0.053 \pm 0.029$; $P < 0.0001$ *vs.* unanesthetized) with high-frequency dynamics that are even further restricted. Principal component analysis of unanesthetized neuronal activity reveals distinct structure corresponding to known behavioral states. At 4% and 8% isoflurane this structure is lost and replaced with randomized dynamics, as quantified by the percentage of total ensemble variance captured by the first three principal components. In unanesthetized worms, this captured variance is high ($88.9 \pm 5.4\%$), reflecting a highly organized system, falling significantly at 4% and 8% isoflurane ($57.9 \pm 11.2\%$, $P < 0.0001$ *vs.* unanesthetized, and $76.0 \pm 7.9\%$, $P < 0.001$ *vs.* unanesthetized, respectively) and corresponding to increased randomization and collapse of system-wide organization.

Conclusions: Anesthesia with isoflurane in *C. elegans* corresponds to high-frequency randomization of individual neuron activity, loss of coordination between neurons, and a collapse of system-wide functional organization.

(*ANESTHESIOLOGY* 2020; 133:133–44)

*C*aenorhabditis elegans is well established as an animal model for the study of volatile anesthetics, displaying distinct stages of behavior under progressively deeper levels of anesthesia.[1] *C. elegans* has also been used to identify genetic mutations that alter mammalian susceptibility to anesthetics,[2,3] demonstrating the evolutionarily conserved nature of the response to volatile anesthetics. In previous work,[4] we established *C. elegans* as a model for imaging neuronal function at the level of multiple, individual neurons under anesthesia. Five command interneurons that control movement behavior in worms within a stereotyped neural circuit were imaged with single-cell resolution using confocal microscopy to investigate the effects of isoflurane on their functional, interrelated activity. Induced dyssynchrony between the neurons in this network was found to be a hallmark of the state of anesthesia, rather than suppression of neuronal activity itself. It was also possible to quantify this state directly using neuron-to-neuron correlations and

---

entropic measures such as mutual information[5] to identify breakdown in the ordered behavior of this subcircuit. These results nevertheless left open the question of whether these observed effects would be conserved throughout the entire nervous system. To address this question requires fast volumetric imaging.

A novel volumetric optical technique, light sheet microscopy, now allows activity to be imaged across the majority of neurons in the animal's head with single-cell resolution while maintaining an appropriate speed to capture neuronal dynamics. In the present work, light sheet microscopy is used to investigate patterns of activity in 120 individual neurons simultaneously at progressively deeper levels of isoflurane anesthesia. Specifically, the isoflurane-induced dyssynchrony that was previously observed within a simple five-neuron subcircuit is found to also hold true when considering the behavior of the majority of the neurons in the head region of *C. elegans*, and a similar progression in neuronal dynamics from synchrony to dyssynchrony to suppression occurs with deepening anesthetic.

In contrast to electroencephalography (EEG), which represents the synchronized fluctuations of many neurons on average, panneuronal imaging allows the activity of individual neurons to be measured, including their absolute state of activation. Consequently, under deep anesthesia, neurons can be identified whose activity pattern would appear as isoelectric on EEG that are not off but instead appear stuck at some intermediate level and are unable to change state further. At moderate levels of anesthesia, high-frequency activity is present as individual neurons appear to become qualitatively jittery and disordered, as if there is no longer a mutually consistent state into which the neuronal system can settle. This particular high-frequency activity is only apparent when the activity of individual neurons can be seen; this signal is lost when neurons are averaged together. In taking this deeper look inside the neuronal state under anesthesia in *C. elegans*, new statistical descriptors must be developed to characterize the changes that occur. Given the hypothesis that anesthesia results from a breakdown in interneuron communication, we look for tractable statistical hallmarks of a loss of organization or structure in the gross activity of hundreds of individual neurons.

Materials and Methods

Strains

C. elegans strains were cultivated at 20°C following standard procedures (on Nematode Growth Media agar seeded with *Escherichia coli* OP50 as a food source). All imaging experiments were performed on young adult hermaphrodites, using the transgenic strain QW1217 (*zfIs124[Prgef-1::G-CaMP6s]; otIs355[Prab-3::NLS::tagRFP]*) expressing panneuronal GCaMP6s and nuclear-localized Red Fluorescent Protein (RFP) in all neurons in the worm (gift of M. Alkema, University of Massachusetts, Worcester, Massachusetts;

fig. 1A). Under the terms of the Animal Welfare Act and the Health Research Extension Act, research involving the use of the invertebrate *C. elegans* is exempt from International Animal Care and Use Committee review.

Imaging Preparation

C. elegans were prepared for imaging following a protocol for encapsulation within a permeable hydrogel.[6] Worms were dipped for 1 to 2 min in 5 mM tetramisole to immobilize them, then placed into 3 μl of a solution of 13.3% polyethylene glycol diacrylate (Advanced BioMatrix, USA) with 0.1% Irgacure (Sigma–Aldrich, USA) on a glass coverslip between two spacers 200 μm in height. A glass slide was placed atop the spacers, and the assemblage was exposed to ultraviolet light, hardening the hydrogel into a flexible and permeable disk and encapsulating the alive worm. This hydrogel disk was secured to a fresh glass slide with low viscosity cyanoacrylate ester (Permabond, USA), and mounted within a 50-mm Petri dish with vacuum grease. The Petri dish was immediately filled with 50 ml of 1× S-Basal solution (100 mM NaCl, 50 mM KPO_4 buffer, 5 μg/ml cholesterol) and 5 mM tetramisole.

Light Sheet Imaging

Each worm was imaged using a Dual Inverted Selective Plane Illumination microscope (Applied Scientific Instrumentation, USA). Imaging was performed with a water-immersed 0.8 NA 40× objective (Nikon, USA) for 5 min, with illumination interleaved between a 488-nm laser at 5 mW power to excite GCaMP6s in the green and a 561 nm laser at 5-mW power to excite NLS::tagRFP in the red (Vortran Laser Technology, USA). Volumetric stacks (41 slices, voxel size 0.1625 μm × 0.1625 μm × 1 μm) in two colors were obtained at two volumes/second for 5 min, producing 49,200 images per session. *C. elegans* neurons typically display slow transient changes in activity rather than rapid action potentials.[7,8] A volume acquisition rate of two volumes per second was sufficient to capture neuron dynamics while limiting photobleaching of the fluorescent markers. Imaging sessions were performed at 0%, 4%, and 8% isoflurane at $t = 30$ min, 150 min, and 270 min, respectively, from the beginning of the imaging experiment. To change isoflurane levels, the existing 1× S-Basal solution was removed from the Petri dish by suction and replaced with an equal volume of fresh buffer containing 5 mM tetramisole and instilled liquid isoflurane (13 μl and 26 μl to begin equilibration to 4% isoflurane and 8% isoflurane, respectively). The Petri dish was then covered and allowed, over the course of the intervening time between imaging sessions, to come to equilibration with an atmosphere of either 4% or 8% isoflurane as maintained with a syringe pump (Harvard Apparatus, USA) and an infrared spectrometer (Ohmeda 5250 RGM, GE Healthcare, USA) at a controlled temperature of 20°C as previously
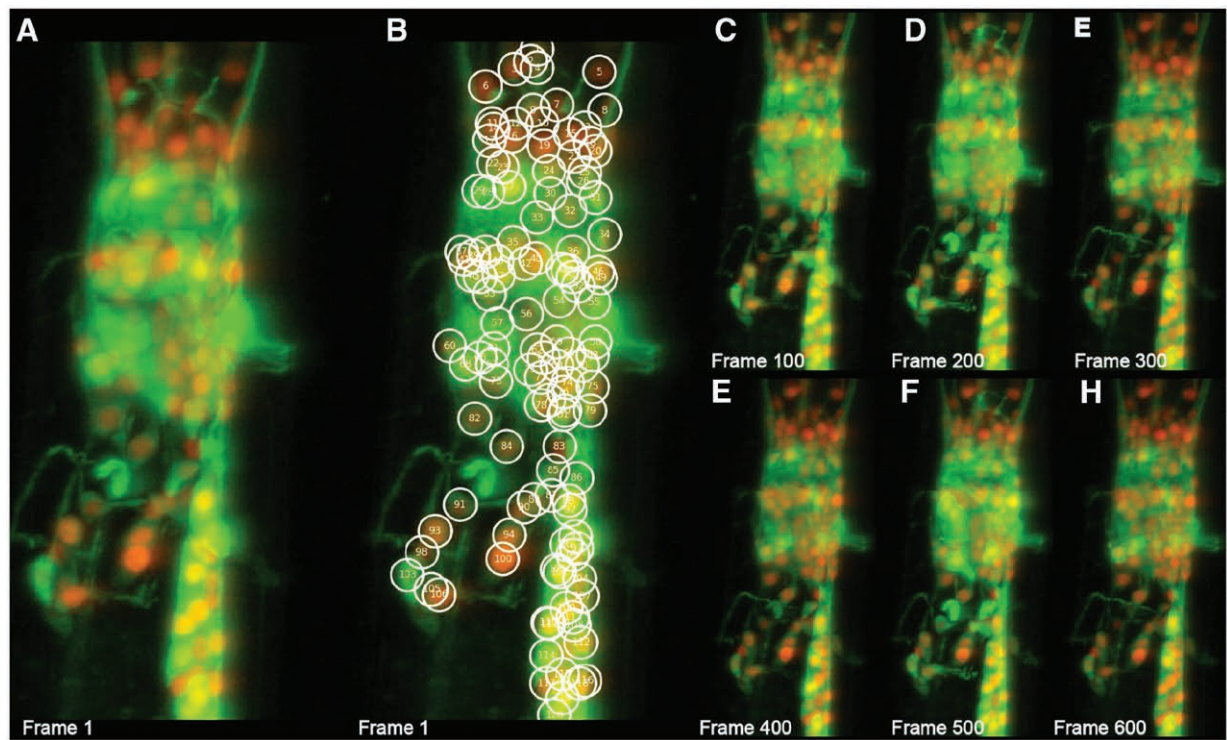
Fig. 1. Multineuron imaging and tracking in the head region of panneuronally labeled *Caenorhabditis elegans* (QW1217) over time. Images are of three-dimensional volumetric data rendered in two dimensions by Maximum Intensity Projection along the *z* axis. (*A*) Image of *C. elegans* head region *via* light sheet imaging. (*B*) As in (*A*), but nuclei tracked for automated signal extraction are displayed. Nuclei are tracked in all three dimensions, but shown here in two-dimensional projection. (*C* through *H*) Select frames from a single imaging trial, showing variation in GCaMP6s fluorescence (*green*), which reports neuronal activity.

described.[4] Ten worms were imaged in this fashion which, based on previous experience[4] and the known profound effects of volatile anesthetics, was expected to be sufficient to yield statistically significant results. Control experiments were also performed in a total of five worms, in which specimens were immobilized and imaged over an identical time schedule, but without the application of any isoflurane. These controls are necessary to separate the effect of anesthetic exposure from any effects attributable to prolonged encapsulation and imaging.

Pharmacology

Previously,[4] 3% isoflurane was identified in nonimmobilized specimens as the concentration at which approximately 50% of worms no longer responded to sharp touch, and this concentration is therefore analogous to a minimum alveolar concentration (MAC) level for a surgical plane of anesthesia in *C. elegans*. Four percent isoflurane then represents 1.33 MAC, a moderate depth of anesthesia sufficient that all of the imaged specimens can be expected to be consistently anesthetized. Eight percent isoflurane represents 2.66 MAC, a deep level of anesthesia.

To assay whether the action of isoflurane is representative of the broader class of highly fluorinated ethers, imaging was repeated with sevoflurane in three specimens. In accordance with the Meyer–Overton hypothesis, sevoflurane concentrations were calculated by scaling according to MAC equipotencies between isoflurane and sevoflurane established in humans.[9] Imaging was performed at sevoflurane concentrations of 0%, 6.6%, and 13.2%. Equilibration to 6.6% and 13.2% was facilitated by instilling 8.5 μl and 17 μl; of liquid sevoflurane, using temperature-adjusted aqueous partition coefficients.[10] Sevoflurane is a more challenging agent to handle for experimental purposes than isoflurane. Its lower potency requires concentrations close to the upper limits of measurement of clinical infrared spectrometers, and its lower aqueous solubility (though desirable for clinical care) results in a less stable experimental preparation as a result of increased off-gassing.

Statistical Methods

Statistical Methods for Neuron Tracking and Extraction of Activity. Approximately 250 Gb of storage was required to hold the total of 147,600 images that were acquired for

each worm. For each 250 Gb volumetric time-series data-set, the nuclei were localized in the red channel *via* the nuclear expression of Red Fluorescent Protein. The localization and tracking of neuronal nuclei follows the overall structure of the method described in Nguyen *et al.*,[11] with modifications suitable for *C. elegans* specimens whose gross movement has been restricted by encapsulation, and in whom the imaging field is restricted to the head only, rather than the entire body. Using the red channel data, a set of implicit axes was created with the origin at the centroid of the data, aligned orthogonally using the second-order moments of the data. Such axes automatically move and turn to compensate for translation or rotation of the head of the worm, stabilizing the tracking. Centerpoints of each nucleus were identified by convolving the red channel data with a Laplacian–of–Gaussian function,[12] picking out nuclei by identifying bright spheres of a critical radius[13] such that 120 neurons in the head were tracked (fig. 1B). Neurons were numbered in the direction of nose to tail, which reflects a general progression of function in the *C. elegans* head from sensory neurons to interneurons to motor neurons. Matching of neurons from one timestep to another was performed using the Kuhn–Munkres Assignment algorithm,[14] always selecting the match that best minimizes the total squared distance between neuron positions. The identified locations of the nuclei were error-corrected using smoothing and consensus based on the location of the surrounding neurons.[11] Ultimately, a single complete chain of locations was established for each of 120 initially identified nuclei from the beginning to the end of each 600-volume image session (fig. 1, C–H). Nuclei were matched across imaging sessions (*i.e.*, from 0% to 4% isoflurane, and from 4% to 8% isoflurane) by a similar technique, by finding the best match from any volume in the first session to any volume in the subsequent session. This matching was performed in a massively parallel computation over many hours (Massachusetts Green High Performance Computing Center, USA). Tracking and extraction algorithms were written in Python, with inner-loop optimization in C.

After the three-dimensional locations of the nuclei of the neurons were established at each time step, their activity was extracted by averaging the somatic GCaMP signal in the green channel in a corona around the nucleus. On rare occasions, a nucleus of one of the tracked neurons would temporarily exit the imaging volume because of motion of the worm. Brief episodes of missing activity data were recovered by cubic interpolation between the activities recorded immediately before and after such events. Such reconstructions were extremely rare, accounting for only 0.0012% of the total data acquired.

Statistical Methods for Analysis of Activity. All statistical analyses were performed using custom MATLAB (Mathworks, USA) scripts as described.

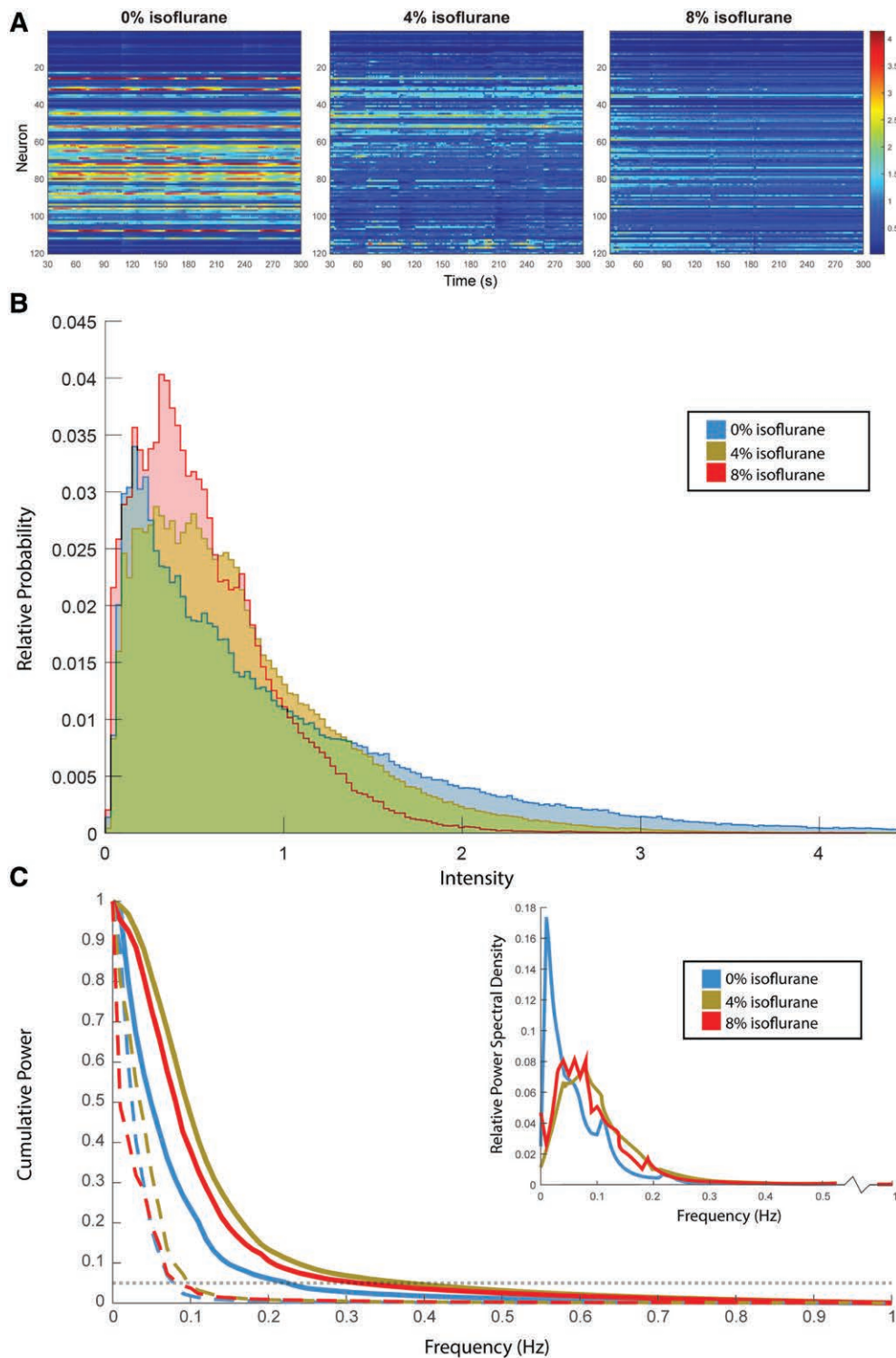Intensity Traces. Intensity traces (fig. 2A) were created by plotting normalized GCaMP fluorescence for each neuron, normalized against the average intensity over all measurements (*i.e.*, all neurons and frames) in the 0% isoflurane session for that worm. The fluorophores fluoresce exuberantly on first illumination; the first 30 s of recorded activity are therefore discarded so that this period does not overwhelm the subsequent analysis.

Activity Distributions. Activity distributions (fig. 2B) were generated as probability histograms of all normalized fluorescence measurements (as above) pooled across all worms, neurons, and frames at each level of isoflurane exposure.

Power Spectral Density. The mean power spectral density across all worms was calculated for each level of isoflurane exposure. The time differential of the normalized fluorescence measurements (as above) was obtained using total-variation regularization,[15] and the power spectral density was calculated by Fourier transformation for each neuron. To mitigate systematic differences between worms in the expression levels of fluorescent markers, the total signal power was normalized for each worm. The mean power spectral density for each level of isoflurane was then produced by averaging over all worms and neurons (fig. 2C). Cumulative power spectral densities were calculated from these mean power spectral densities. Bulk power spectral density measurements for each worm were produced by averaging the fluorescence measurements of all neurons within that worm.

Neuron Activity Correlations. Neuron–neuron correlations were taken between the time differential of signals for each neuron–neuron pair (fig. 3A), as in Awal *et al.*[4] Mean correlations were calculated by averaging the correlation for all neuron–neuron pairs for each worm at each level of isoflurane exposure, then averaging across all worms. Pearson correlation distributions (fig. 3B) were generated from probability histograms of all correlation measurements pooled across all worms at that level of isoflurane exposure. Mean correlation values were taken from these distributions and statistical tests assessed by a one-way ANOVA, followed by paired two-tailed *t* tests. Tukey adjustment for multiple comparisons was applied to assess significance between groups.

Principal Component Analysis. Principal component analysis was performed on the normalized fluorescence measurements (normalized to the mean intensity of the 0% isoflurane session, as above) for all 120 neurons in all worms. Principal component analysis plots (fig. 4A) were generated by plotting the value of the first three principal components on Cartesian axes over time. The color of the principal component analysis trace reports the intensity of the AVA neuron using the same color scheme as figure 2A. AVA is the standard name of one of the more readily–identifiable neurons in *C. elegans* based on anatomic location and activity. AVA is a command interneuron which governs locomotion reversal. It performs something broadly analogous to a cerebellar function: When AVA is activated, downstream neuronal activity is modulated such that the worm moves

Fig. 2. Neuronal activity distributions and spectral analysis. (*A*) Intensity trace of fluorescence activity of all 120 tracked neurons in an individual *Caenorhabditis elegans* at 0% (*left*), 4% (*middle*), and 8% (*right*) isoflurane. The color scale covers 0% to 75% of the dynamic range of the normalized intensities to remove rare high-level activations and render lower-level activity in a more discernable fashion. The time range covers 30 to 300 s, to exclude exuberant fluorescence caused by initial illumination. (*B*) Distribution of all fluorescence measurements pooled across all neurons and worms at each level of isoflurane exposure. (*C*) Mean cumulative power spectral densities of neuron fluorescence signals at each level of isoflurane exposure. Cumulative power spectral densities for bulk fluorescence measurements in *dashed lines*. The 95% spectral edge shown is shown with a *dotted gray line*. (*Inset*) Mean power spectral density of neuron fluorescence signals at each level of isoflurane.
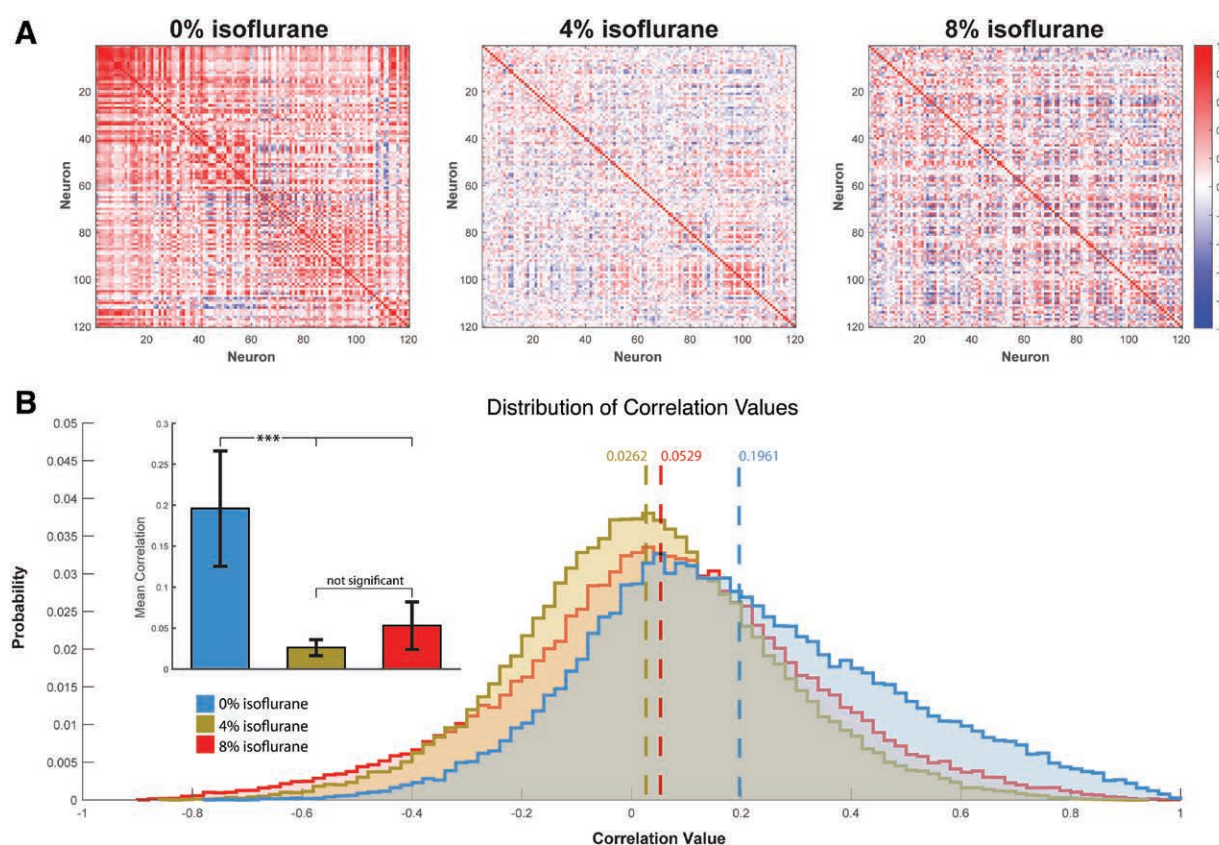
Fig. 3. Neuronal correlations. (*A*) Correlation of fluorescence signals for each neuron–neuron pair from the intensity traces in figure 2A at 0% (*left*), 4% (*middle*), and 8% (*right*) isoflurane. The color scale is red when a correlation exists, blue when anticorrelated, and white when no correlation is found. The leading diagonal is red because each neuron is correlated to itself by definition. (*B*) Distributions of all correlation values measured at each level of isoflurane. (*Inset*) Mean correlation values at each level of isoflurane. Sample variability reported as SD. (***$P < 0.0001$).

backwards. In the unanesthetized worm, the activation state of AVA reliably discriminates the neurologically intended direction of movement,[16] even if the worm itself is physically immobilized or pharmacologically paralyzed.[17] The AVA neuron was manually identified in the 0% isoflurane session by morphology and activity, and in following sessions by morphology and spatial consistency; its activity values were extracted from the larger dataset.

Percentage variance was calculated as the percentage of the total variance in the data that was captured by the first three principal components. Percentage variance was calculated for each worm at each trial, then averaged across worms and assessed by a one-way ANOVA, followed by paired two-tailed *t* tests. Tukey adjustment for multiple comparisons was applied to assess significance between groups.

Results

Neuronal Imaging

A dual inverted selective plane illumination microscope was used to generate three-dimensional volumetric time-lapse images of the head-region of *C. elegans* panneuronally expressing two fluorophores: a nuclear-localized Red Fluorescent Protein (red), and a cytoplasmically-expressed calcium sensor, GCaMP6s (green; fig. 1A). For each movie, computer-automated image analysis identified the red nuclei of 120 neurons, tracked them over time, and extracted the surrounding GCaMP fluorescent signal (fig. 1B). GCaMP is widely used as an optical metric of neuronal activation because it reports the elevated cytoplasmic calcium in response to neuronal activity.[18] By measuring the average green GCaMP fluorescence intensity surrounding a given nucleus, that neuron's activity can be extracted. Figure 1 (C–H) illustrates this, showing individual frames between which the fluorescence of individual neurons can be observed to change. Each worm (n = 10 worms) was imaged at progressively deeper levels of exposure to isoflurane equilibrated to 0%, 4%, and 8% vol/vol respectively, capturing the activity of all of the head ganglia (fig. 1A) which include the majority of all *C. elegans* interneurons. The images shown in figure 1 are two-dimensional representations of the underlying volumetric dataset, with pixel intensities assigned using the
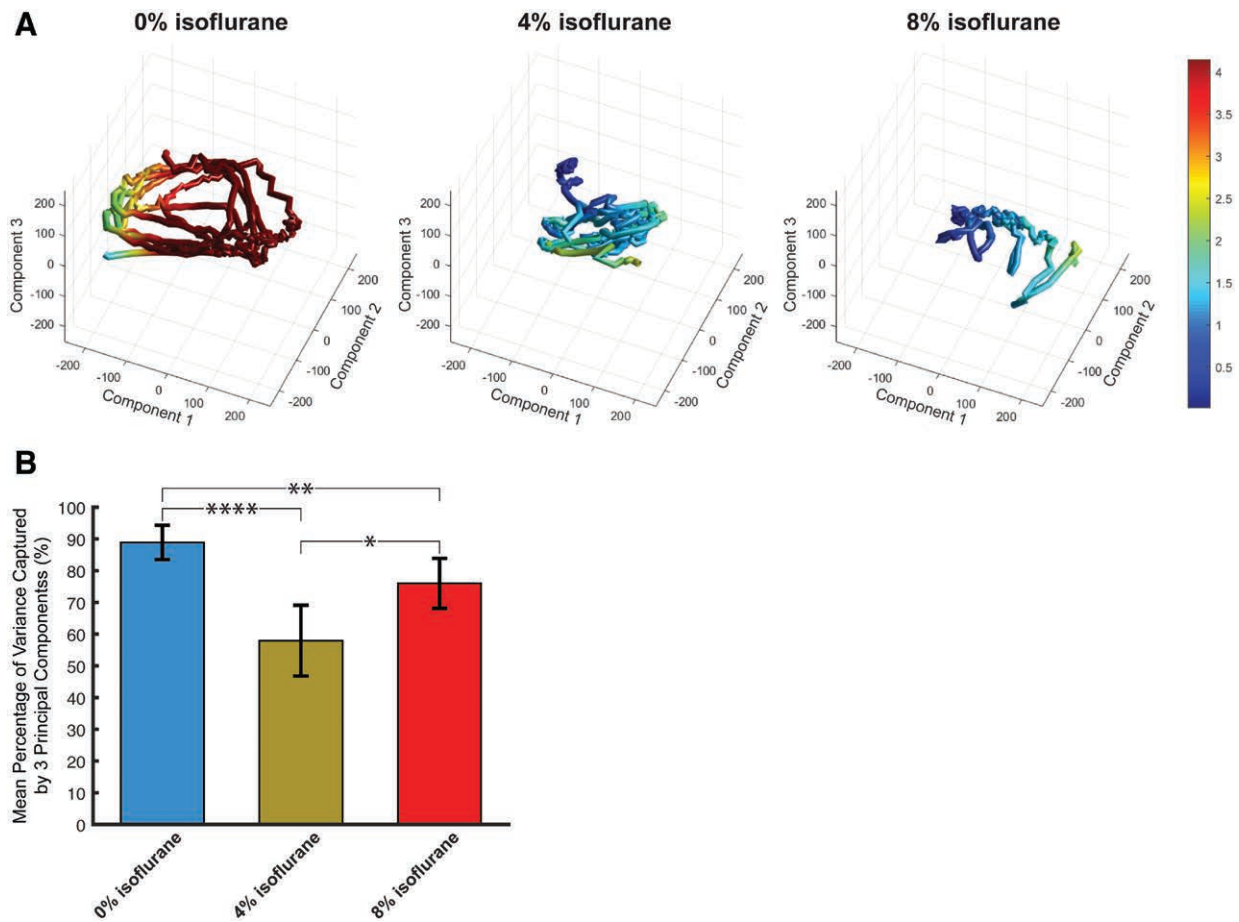
Fig. 4. System-wide activity states. (*A*) Three-dimensional plots of the first three principal components calculated from the 120 individual neuron signals shown in figure 2A at 0% (*left*), 4% (*middle*), and 8% (*right*). Principal component analysis traces are colored by the fluorescence intensity of the neuron AVA, with the same color scale as in figure 2A. (*B*) Mean percentage of total variance captured by the first three principal components for all neurons and for all worms at each level of isoflurane. Sample variability reported as SD. (*P < 0.01; **P < 0.001; ****P < 0.00001).

Maximum Intensity Projection ray-casting algorithm[19] as is commonly performed for positron emission tomography and single photon emission computed tomography images. Figure 2A displays the activity of 120 neurons from a single animal over the course of the three sessions at 0%, 4%, and 8% isoflurane.

At 0% isoflurane, the worm displays its characteristic and innate neural activity in which the nervous system transitions between global activity states corresponding to different gross behavioral activities.[17,20–22] These behavioral state transitions can be observed as the coordinated shifts in activity of large number of neurons over long (*e.g.*, up to 35 s) time intervals (fig. 2A, *left*). At 4% isoflurane, worms no longer respond to stimuli nor exhibit functional locomotive behavior.[4,23] Although substantial individual neuronal dynamics persist at this dosage, ordered activation across many neurons is diminished (fig. 2A, *middle*). At 8%

isoflurane, the GCaMP signals cease to fluctuate and the neurons appear to maintain a low, although not necessarily zero, level of fluorescence (fig. 2A, *right*).

Qualitatively, it is clear that high doses of isoflurane do profoundly suppress neuronal dynamics. However, as noted previously,[4] this profound suppression is not seen at 4% isoflurane, even though response to stimulus and locomotive behavior are already lost at this level. Instead, it is the coordination between large numbers of neurons, obvious in worms at 0% isoflurane, which is lost with the onset of anesthesia.

These observations are reflected in the activity distribution across trials. For each level of exposure to isoflurane, all GCaMP fluorescence intensity measurements across all worms and neurons were pooled and plotted (fig. 2B). Worms at 0% isoflurane (fig. 2B, *blue*) have activity distributions that extend across the entire dynamic range from zero

fluorescence to very high GCaMP fluorescence. At 4% isoflurane (fig. 2B, *yellow*), measurements at higher levels of fluorescence are dramatically decreased whereas measurements of middle and lower levels of fluorescence increase. At 8% isoflurane (fig. 2B, *red*), the distribution is further restricted to lower, but notably nonzero, fluorescence.

Spectral Analysis

Drawing on classical statistical hallmarks of anesthesia in humans,[24] a power spectral analysis of the fluorescence signals measured from individual neurons was performed. Figure 2C shows the cumulative average power spectrum of all neurons (across all worms) at each level of isoflurane. The corresponding mean power spectral densities for each condition are displayed in the inset. Both 4% isoflurane (fig. 2C, *yellow*) and 8% isoflurane (fig. 2C, *red*) are shifted toward higher frequencies compared with that of worms at 0% isoflurane. These shifts can be quantified by measuring the 95% spectral edge frequency, defined as the frequency below which 95% of the total signal power resides. As illustrated in figure 2C (*dotted gray line*), the 95% spectral edge is 0.23 Hz, 0.38 Hz, and 0.32 Hz for 0%, 4%, and 8% isoflurane, respectively. This shift in power spectral densities toward higher frequencies summarizes the changes in neuronal dynamics noted above (fig. 2A), in which large numbers of neurons that display extended periods of activation and deactivation at 0% isoflurane transition to randomized and rapid dynamics under anesthesia.

Averaging the fluorescence signals of all 120 neurons tracked in an individual worm serves as a measure of bulk neuronal activity for that animal. Such bulk measurements are conceptually similar to those of EEG measurements in humans, in which measurements of neuronal activity are made over ensembles of many thousands to millions of neurons in particular locations in the brain. The cumulative power spectral densities of these bulk measurements (fig. 2C, *dashed lines*) are shifted toward lower frequencies, with 95% spectral edges of 0.08 Hz, 0.10 Hz, and 0.09 Hz at 0%, 4%, and 8% isoflurane, respectively. These bulk measurements therefore fail to capture the shift toward high-frequency dynamics under anesthesia that is clearly apparent in measurements made with single neuron resolution.

Neuronal Correlation. The degree of coordination within the nervous system can be estimated by calculating the activity correlations between neuron pairs. Figure 3A shows the correlation between fluorescence signals in all neuron–neuron pairs for each level of isoflurane for the intensity data displayed in figure 2A. Globally, there is a clear decrease in neuron–neuron correlation (*i.e.*, whiter) at 4% isoflurane compared with 0% isoflurane. At 8% isoflurane, GCaMP signals display marked reductions in fluctuation and hence correlations increase to some degree owing to stasis.

At 0% isoflurane, the distribution of correlations is skewed toward positive correlation, whereas the distributions at 4% and 8% are more symmetrically distributed

around zero (*i.e.*, no correlation; fig. 3B). This observation is quantified by calculating the mean correlation between all neuron pairs and across all animals at each level of isoflurane (fig. 3B, *inset*). The mean interneuronal correlation is high at 0% isoflurane ($R = 0.196 \pm 0.070$ relative units), but drops significantly at 4% and 8% isoflurane ($R = 0.026 \pm 0.010$ relative units and $R = 0.053 \pm 0.029$ relative units, respectively; $P < 0.0001$). The observed drop in correlation between neurons is reflective of a general breakdown in coordinated signaling between neurons during anesthesia.

Principal Component Analysis

The system–wide neuronal activity in the ganglia of the worm head can be analyzed using principal component analysis.[17,21] Principal component analysis efficiently reduces large dimensional data sets to fewer principal components while retaining most of the dynamic information. The independent activity of 120 neurons can be easily reduced and visualized on Cartesian axes by plotting the first three principal components. Figure 4A shows the principal component analysis representation of the intensity activity data shown in figure 2A. At 0% isoflurane (fig. 4A, left), there is a clear oscillation in system activity that effectively traces a loop in the principal component analysis state space. To compare the principal component analysis state space with the gross behavioral state of the system, the principal component analysis activity trace is colored by the fluorescence intensity measured from the interneuron AVA over time. AVA is a key command interneuron whose activity strictly corresponds to the direction of the worm's crawling state.[25] When AVA activity is high (*i.e.*, high GCaMP fluorescence and red principal component analysis trace color), the animal is attempting to reverse and when AVA activity is low (*i.e.*, low fluorescence and blue and green principal component analysis trace color), the animal is attempting to crawl forward.

As shown in figure 4A, AVA activity and therefore the gross behavior state clearly correspond with position in the principal component analysis state space at 0% isoflurane. At 4% isoflurane, in contrast, the regular oscillations within principal component analysis state space collapse. The activity trace dynamics become randomized but do not fall to a specific point. These results indicate that neuronal activity remains but that the overall structure and regularity of the system dynamics are lost. Moreover, AVA fluorescence (as represented by trace color) no longer corresponds to particular locations in the principal component analysis state space, further indicating disruption of well-defined neuronal states. At 8% isoflurane, the principal component analysis space collapses further, as neuronal dynamics decrease overall.

The percentage of total variance in the data (*e.g.*, the dynamic change in the data) that can be captured by the first three principal components serves as a general metric for the degree of independence between measured variables

in the system. If the distinct measurements (*i.e.,* fluorescence measurement of each neuron) are highly dependent on one another, then the state of the system can be adequately summarized through only a few independent principal components. The average variance captured by the first three principal components across all worms at each level of isoflurane (fig. 4B) was calculated: 88.9% ± 5.4% at 0% isoflurane, falling to 57.9% ± 11.2% at 4% isoflurane, and rising to 76.0% ± 7.9% at 8% isoflurane. Each of these group measurements is significantly different from the others (0% isoflurane *vs.* 4% isoflurane, $P < 0.0001$; 0% isoflurane *vs.* 8% isoflurane, $P < 0.001$; 4% isoflurane *vs.* 8% isoflurane, $P = 0.001$). The principal component analysis–based technique discriminates the effects of isoflurane and is far more computationally efficient than the entropic and Mutual Information statistical methods previously used.

Control Experiments

Control experiments performed using five worms and tracking 120 neurons without isoflurane exposure demonstrated only small and nonsignificant changes in these statistical properties, as illustrated in Supplemental Digital Content 1 (http://links.lww.com/ALN/C351). Consequently, we conclude that the effects ascribed to isoflurane exposure do arise from exposure to the volatile anesthetic agent rather than the experimental process of encapsulation and imaging.

Comparative Pharmacodynamics of Sevoflurane and Isoflurane

Supplemental Digital Content 2 (http://links.lww.com/ALN/C352) shows the intensity traces of the fluorescent activity of 120 tracked neurons under exposure to sevoflurane at 0%, 6.6%, and 13.2% over three trials, in the manner of figure 2A. A similar activity pattern of structure, disorder, and suppression exists under increasing concentrations of sevoflurane, as would be expected from the isoflurane results. Principal component analysis also shows a considerable fall in the variance captured by the first three principal components at 6.6% sevoflurane, as was also found at 4% isoflurane. These similarities in the statistical action of isoflurane and sevoflurane on the activity of *C. elegans* neurons is suggestive of a common pharmacodynamic or class effect for the highly fluorinated ethers.

Discussion

In this study, sophisticated light sheet microscopy and volumetric image analysis are used to measure the individual activity of the majority of neurons within the *C. elegans* head under progressive exposure to deeper levels of isoflurane anesthesia. These single neuron resolution measurements enable an analysis of system–wide dynamics under anesthesia that has not yet been technically possible. Previously,[4] imaging techniques restricted to a subcircuit of only five

command interneurons were used to demonstrate that the state of anesthesia in worms does not correspond with suppressed activity in those neurons but rather to dyssynchrony within this inherently highly organized circuit. Here, the capacity of these imaging techniques is now expanded to encompass the majority of neurons in the worm's head. The results of these panneuronal experiments are remarkably consistent with those previous subcircuit results, implying that the measured effects of anesthesia are generalizable throughout the animal's entire nervous system.

The activity of neurons in unanesthetized *C. elegans* has been well studied.[16,17,20–22] Unanesthetized *C. elegans* neurons display highly correlated activity across the nervous system, consisting of slow transitions between system–wide activity states. These characteristics are readily observed within the metrics of neuronal activity assessed here. The degree of correlation between neurons is relatively high (fig. 3), whereas the power spectral density analysis of neuron activity displays the majority of power at lower frequencies reflecting the slow transition between activity states (fig. 2). Likewise, the principal component analysis plots (fig. 4A, *left*), which allow visualization of system–wide dynamics, display an organized looping as the system oscillates between activity states. These states, or regions of principal component analysis space, are correlated with activity of the key interneuron AVA that effectively reports the forward and reverse crawling behavioral state of the animal.

At moderate levels of anesthesia (4% isoflurane), the system–wide organization in neuron activity is lost while dynamics of the individual neurons shift to higher frequencies. The increase in system–wide dyssynchrony is evident from the decrease in neuron–neuron correlation (fig. 3), as well as the loss of structure and reduced percentage variance captured by the principal component analysis trace (fig. 4A, *middle*). Critically, these effects are not the result of simple suppression of neuron activity; rather, individual neurons remain active as illustrated by the pooled neuron fluorescence distribution in figure 2B, which narrows to mid–range but nonzero fluorescence (*i.e.*, activity). Likewise, the shift of the mean power spectral density to higher frequencies at 4% isoflurane (fig. 2C) indicates increased rapid fluctuations in individual neuronal activity as the slow transitions between system–wide neuronal states are lost. Thus, as also found within the interneuron subcircuit,[4] the state of anesthesia appears to stem from randomization of individual neuron activity leading to increased dyssynchrony and thus loss of functional organization across the entire nervous system. The fall in total percentage variance captured in the principal component analysis is consistent with the rise in Shannon information entropy seen in the interneuron subcircuit[4] as the disorder increases.

At deeper levels of anesthesia (8% isoflurane) increased suppression of neuron dynamics is observed, accompanied by continued loss of organized system–wide activity. This is evident by the pooled activity distribution in figure 2B

that illustrates a further restriction of the neuronal dynamic range around moderately low activity levels. Likewise, the principal component analysis plot at 8% isoflurane continues to display a lack of organized structure (fig. 4A, *right*). Although neuron–neuron correlation and percentage variance represented by the principal component analysis plots increase moderately over measurements at 4% isoflurane, this is most likely attributable to the uniform suppression of all neuronal dynamics, thereby making them more uniformly correlated, rather than a property of the individual neuron activity. Importantly, during deep anesthesia, the neurons do not appear to simply turn off but instead enter a period of stasis in which neuronal state transitions no longer occur. Thus, as the neuronal dynamics decrease they appear to become increasingly constrained to fixed moderate-to-low levels of activity. Anesthesia in humans is also associated with increased phase coupling of activity across brain regions;[26–29] it appears a similar effect can be observed across the *C. elegans* nervous system as the activity of individual neurons becomes locked.

In humans, measurements of anesthetic depth are derived from EEG measurements, which constitute bulk average electrical measurements across many thousands of pyramidal neurons over comparatively large regions of the brain. For an EEG signal to be detectable with a scalp electrode, it must synchronize approximately $6\,cm^2$ of cortical surface.[30,31] It is therefore constructive to compare the measurements obtained at single neuron resolution to a mean fluorescence signal obtained by averaging *a priori* across the measurements of all 120 individual neurons in each worm (*i.e.*, the fluorescence equivalent of an averaged bulk measurement similar to that of an EEG). As seen in figure 2C (*dashed lines*), these bulk fluorescence signals lack high frequency dynamics in the resulting power spectrum: No difference is seen in the cumulative power spectral density of the bulk fluorescence measurements at 0%, 4%, and 8% isoflurane exposure, in contrast to the large shifts observed in the power spectrum of single neuron measurements. The effects of isoflurane on the high-frequency dynamics of individual neurons are effectively averaged out and cannot be discerned by bulk measurement.

As we found previously within the small subcircuit of command interneurons, the onset of anesthesia in *C. elegans* corresponds to a state of increased randomization and dyssynchrony between neurons rather than a generalized silencing of neuronal activity. This study demonstrates these effects across the majority of interneurons in the animal's nervous system and further illustrates the shortcomings of bulk neuronal measurements for measuring such effects. The nervous system of *C. elegans* is not sufficiently complex to be able to develop the consistent patterns of rhythmic excitation that are the hallmarks of EEG; nevertheless, *C. elegans* becomes anesthetized on exposure to volatile anesthetics. This discrepancy highlights the difference between the well-characterized macroscale effects of isoflurane on

measurements such as EEG, and the microscale effects on neuronal circuits that are still relatively unknown. The neuronal state of isoflurane anesthesia in *C. elegans* appears different from that seen in, for example, the inactivity and reduced responsiveness of sleep (*lethargus*).[21]

Recent exciting advances in *C. elegans* biology include, first, the development of an animal with unique patterns of multiple fluorophores in each nucleus,[32] rather than the single panneuronal promoter of Red Fluorescent Protein used here. This polychromatic labeling allows neurons to be identified automatically and explicitly, without having to rely on anatomical geometry and known patterns of activation in the unanesthetized animal. Second, new electron micrograph sections of *C. elegans* have now established the connectome matrices for all neuron-to-neuron chemical synapses and gap junctions in both the hermaphroditic and male sexes.[33] Taken together, these advances will allow the analysis of the effects of anesthetics on specific neuronal types, neural circuits, and sensorimotor pathways within the context of the entire functioning nervous system.

The imaging performed in this study was performed at discrete concentrations of isoflurane during induction, which leaves open a range of questions regarding how neuronal coordination changes in response to, for example, progressive recovery from anesthesia. Would neuronal coordination be expected to recover in a smooth and progressive fashion, or would identifiable step changes occur? Furthermore, even if the underlying neuronal recovery were to occur smoothly, would step changes in particular behavioral endpoints be seen once neuronal coordination rises above some sufficient level? Ultimately, the application of these powerful new multineuron imaging techniques in *C. elegans,* and also in higher animals,[34] will generate a comprehensive understanding of the anesthetic effects on neuronal function and interconnectivity and bridge the gap between our current understanding of the behavioral and clinical effects of anesthetics and their cellular mechanisms of action.

Research Support

Competing Interests

Dr. Connor is a consultant for Teleflex, LLC (Wayne, Pennsylvania), on airway equipment design. This activity is unrelated to the material in this manuscript. The remaining authors declare no competing interests.

Correspondence

Address correspondence to Dr. Connor: Department of Anesthesiology, Perioperative and Pain Medicine, Brigham and Women's Hospital, 75 Francis Street, CWN L1,

Boston, Massachusetts 02115. cconnor@bwh.harvard.edu. Information on purchasing reprints may be found at www.anesthesiology.org or on the masthead page at the beginning of this issue. ANESTHESIOLOGY's articles are made freely accessible to all readers, for personal use only, 6 months from the cover date of the issue.

References

1. Morgan PG, Kayser EB, Sedensky MM: C. elegans and volatile anesthetics (May 3, 2007), Wormbook. Edited by the C. elegans Research Community. Available at: http://dx.doi.org/10.1895/wormbook.1.140.1 or http://www.wormbook.org/chapters/www_anesthetics/anesthetics.html. Accessed March 27, 2020.

2. Quintana A, Morgan PG, Kruse SE, Palmiter RD, Sedensky MM: Altered anesthetic sensitivity of mice lacking Ndufs4, a subunit of mitochondrial complex I. PLoS One 2012; 7:e42904

3. Sedensky MM, Pujazon MA, Morgan PG: Tail clamp responses in stomatin knockout mice compared with mobility assays in Caenorhabditis elegans during exposure to diethyl ether, halothane, and isoflurane. ANESTHESIOLOGY 2006; 105:498–502

4. Awal MR, Austin D, Florman J, Alkema M, Gabel CV, Connor CW: Breakdown of neural function under isoflurane anesthesia: *In vivo*, multineuronal imaging in caenorhabditis elegans. ANESTHESIOLOGY 2018; 129:733–43

5. Studený M, Vejnarová J: The multiinformation function as a tool for measuring stochastic dependence, Learning in graphical models, Springer, 1998, pp 261–97

6. Burnett K, Edsinger E, Albrecht DR: Rapid and gentle hydrogel encapsulation of living organisms enables long-term microscopy over multiple hours. Commun Biol 2018; 1:73

7. Lockery SR, Goodman MB: The quest for action potentials in C. elegans neurons hits a plateau. Nat Neurosci 2009; 12:377–8

8. Mellem JE, Brockie PJ, Madsen DM, Maricq AV: Action potentials contribute to neuronal signaling in C. elegans. Nat Neurosci 2008; 11:865–7

9. Eger EI 2nd: Age, minimum alveolar anesthetic concentration, and minimum alveolar anesthetic concentration-awake. Anesth Analg 2001; 93:947–53

10. Hönemann CW, Washington J, Hönemann MC, Nietgen GW, Durieux ME: Partition coefficients of volatile anesthetics in aqueous electrolyte solutions at various temperatures. ANESTHESIOLOGY 1998; 89:1032–5

11. Nguyen JP, Linder AN, Plummer GS, Shaevitz JW, Leifer AM: Automatically tracking neurons in a moving and deforming brain. PLoS Comput Biol 2017; 13:e1005517

12. Russ JC, Neal FB: Image enhancement in the spatial domain, The Image Processing Handbook, Seventh edition. Boca Raton, CRC Press, Taylor & Francis Group, 2016, pp xvii, 1035 pages

13. Huertas A, Medioni G: Detection of intensity changes with subpixel accuracy using laplacian-gaussian masks. IEEE Trans Pattern Anal Mach Intell 1986; 8:651–64

14. Jonker R, Volgenant A: A shortest augmenting path algorithm for dense and sparse linear assignment problems. Computing 1987; 38: 325–340

15. Chartrand R: Numerical differentiation of noisy, nonsmooth data. ISRN Applied Mathematics 2011; 2011:e164564

16. Gray JM, Hill JJ, Bargmann CI: A circuit for navigation in Caenorhabditis elegans. Proc Natl Acad Sci USA 2005; 102:3184–91

17. Kato S, Kaplan HS, Schrödel T, Skora S, Lindsay TH, Yemini E, Lockery S, Zimmer M: Global brain dynamics embed the motor command sequence of Caenorhabditis elegans. Cell 2015; 163:656–69

18. Chen TW, Wardill TJ, Sun Y, Pulver SR, Renninger SL, Baohan A, Schreiter ER, Kerr RA, Orger MB, Jayaraman V, Looger LL, Svoboda K, Kim DS: Ultrasensitive fluorescent proteins for imaging neuronal activity. Nature 2013; 499:295–300

19. Wallis JW, Miller TR: Three-dimensional display in nuclear medicine and radiology. J Nucl Med 1991; 32:534–46

20. Nguyen JP, Shipley FB, Linder AN, Plummer GS, Liu M, Setru SU, Shaevitz JW, Leifer AM: Whole-brain calcium imaging with cellular resolution in freely behaving Caenorhabditis elegans. Proc Natl Acad Sci USA 2016; 113:E1074–81

21. Nichols ALA, Eichler T, Latham R, Zimmer M: A global brain state underlies C. elegans sleep behavior. Science 2017; 356 (6344), eaam6851

22. Venkatachalam V, Ji N, Wang X, Clark C, Mitchell JK, Klein M, Tabone CJ, Florman J, Ji H, Greenwood J, Chisholm AD, Srinivasan J, Alkema M, Zhen M, Samuel AD: Pan-neuronal imaging in roaming Caenorhabditis elegans. Proc Natl Acad Sci USA 2016; 113:E1082–8

23. Morgan PG, Cascorbi HF: Effect of anesthetics and a convulsant on normal and mutant Caenorhabditis elegans. ANESTHESIOLOGY 1985; 62:738–44

24. Schwender D, Daunderer M, Mulzer S, Klasing S, Finsterer U, Peter K: Spectral edge frequency of the electroencephalogram to monitor "depth" of anaesthesia with isoflurane or propofol. Br J Anaesth 1996; 77:179–84

25. Roberts WM, Augustine SB, Lawton KJ, Lindsay TH, Thiele TR, Izquierdo EJ, Faumont S, Lindsay RA, Britton MC, Pokala N, Bargmann CI, Lockery SR: A stochastic neuronal model predicts random search

behaviors at multiple spatial scales in C. elegans. Elife 2016; 5:e12572

26. Ferron JF, Kroeger D, Chever O, Amzica F: Cortical inhibition during burst suppression induced with iso-flurane anesthesia. J Neurosci 2009; 29:9850–60

27. Mukamel EA, Pirondini E, Babadi B, Wong KF, Pierce ET, Harrell PG, Walsh JL, Salazar-Gomez AF, Cash SS, Eskandar EN, Weiner VS, Brown EN, Purdon PL: A transition in brain state during propofol-induced unconsciousness. J Neurosci 2014; 34:839–45

28. Pal D, Silverstein BH, Sharba L, Li D, Hambrecht-Wiedbusch VS, Hudetz AG, Mashour GA: Propofol, sevoflurane, and ketamine induce a reversible increase in delta-gamma and theta-gamma phase-amplitude coupling in frontal cortex of rat. Front Syst Neurosci 2017; 11:41

29. Soplata AE, McCarthy MM, Sherfey J, Lee S, Purdon PL, Brown EN, Kopell N: Thalamocortical control of propofol phase-amplitude coupling. PLoS Comput Biol 2017; 13:e1005879

30. Cooper R, Winter AL, Crow HJ, Walter WG: Comparison of subcortical, cortical and scalp activity using chronically indwelling electrodes in man. Electroencephalogr Clin Neurophysiol 1965; 18:217–28

31. Britton JW, Frey LC, Hopp JL, Korb P, Koubeissi MZ, Lievens WE, Pestana-Knight EM, St.Louis EK: The scientific basis of EEG: Neurophysiology of EEG generation in the brain, Electroencephalography (EEG): An introductory text and atlas of normal and abnormal findings in adults, children and infants. Edited by St. Louis EK, Frey LC. Chicago, IL, American Epilepsy Society, 2016

32. Yemini E, Lin A, Nejatbakhsh A, Varol E, Sun R, Mena G, Samuel AD, Paninski L, Venkatachalam V, Hobert O: NeuroPAL: A Neuronal Polychromatic Atlas of Landmarks for Whole-Brain Imaging in C Elegans. BioRxiv 676312; June 2019. Available at: https://doi.org/10.1101/676312. Accessed March 27, 2020.

33. Cook SJ, Jarrell TA, Brittin CA, Wang Y, Bloniarz AE, Yakovlev MA, Nguyen KCQ, Tang LT, Bayer EA, Duerr JS, Bülow HE, Hobert O, Hall DH, Emmons SW: Whole-animal connectomes of both Caenorhabditis elegans sexes. Nature 2019; 571:63–71

34. Wenzel M, Han S, Smith EH, Hoel E, Greger B, House PA, Yuste R: Reduced repertoire of cortical microstates and neuronal ensembles in medically induced loss of consciousness. Cell Syst 2019; 8:467–474.e4.